Chapter 6

Camera/Detector & Images

The characteristics of the camera lens is investigated and combined with the results from the previous chapters to find the overall system matrix, *S*. The theoretical image of the fibre on the detector can then be calculated.

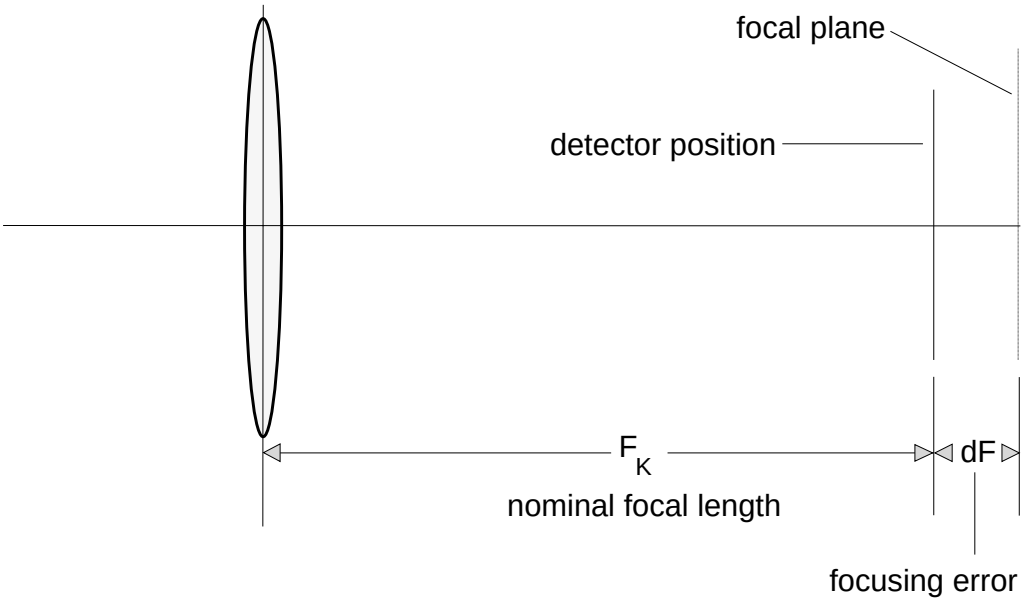

Figure 6.1: Camera lens system with focussing error.

6.1 Camera Matrix K

The component matrix, K, describes the position (and angle) at which an arbitrary ray entering the camera strikes the plane of the detector. As discussed in chapter 4, relative focussing error of up to approximately 0.03% will be assumed. Figure 6.1 illustrates the geometry of a simple camera lens with the principal (or reference) ray coincides with the optic axis.

The path of a light ray entering the camera can be described by a refraction followed by translation. The camera matrix, K, can therefore be derived from:

$$K = T_{(F_k)} R_{(F_k+dF)} \tag{6.1}$$

If we let

$$\varepsilon_k = \frac{dF}{F_k + dF} \tag{6.2}$$

then:

$$K \approx \begin{vmatrix} \varepsilon_k & 0 & F_k & 0 \\ 0 & \varepsilon_k & 0 & F_k \\ \frac{-1}{F_k(1+\varepsilon_k)} & 0 & 1 & 0 \\ 0 & \frac{-1}{F_k(1+\varepsilon_k)} & 0 & 1 \end{vmatrix} \tag{6.3}$$

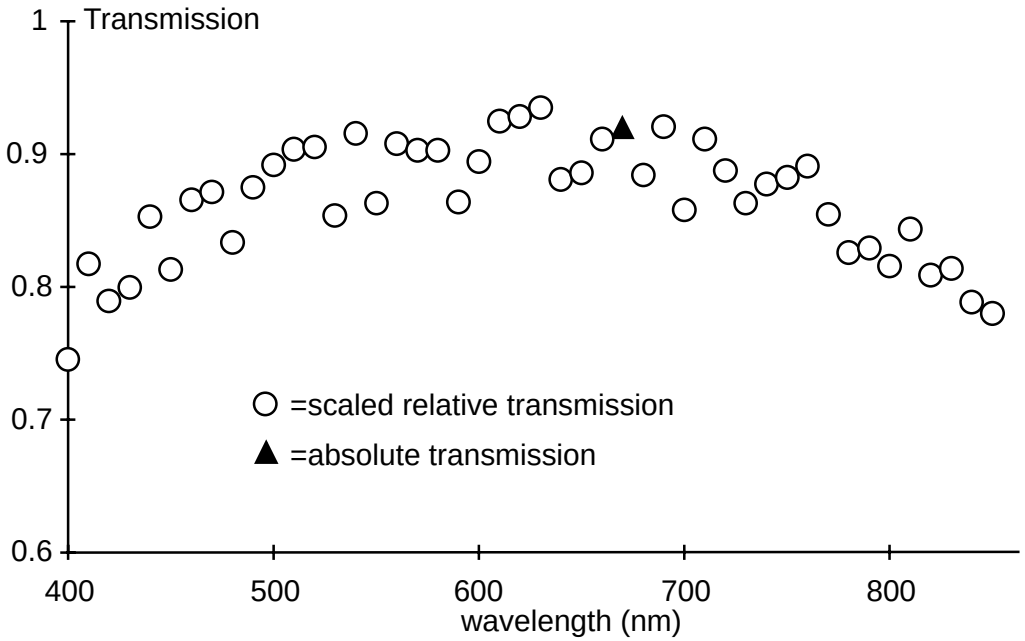

Figure 6.2: Transmission for the 135mm f2.0 Cannon lens.

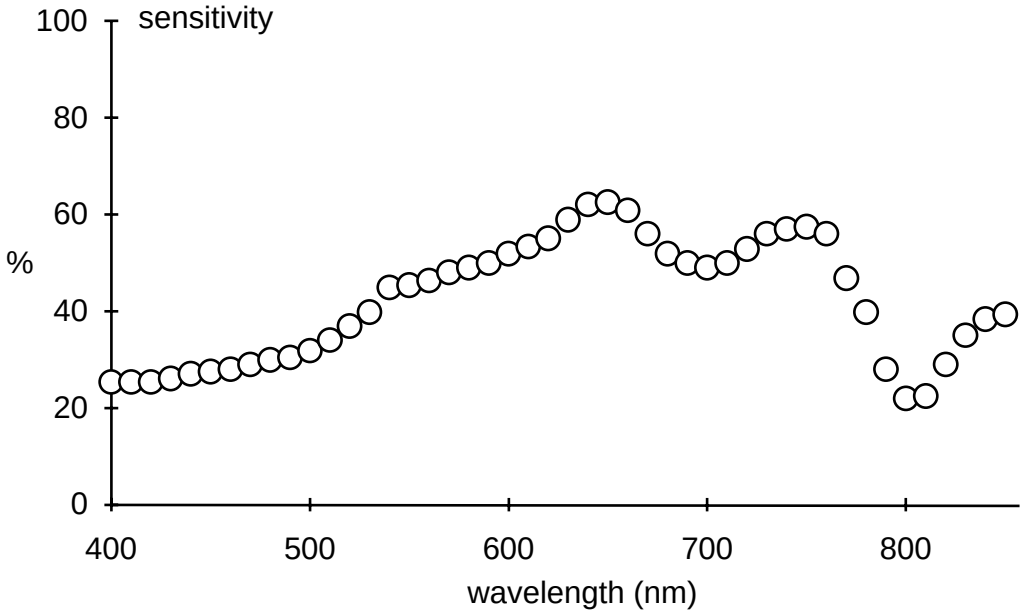

Figure 6.3: Texas Instruments TC215 CCD sensitivity.

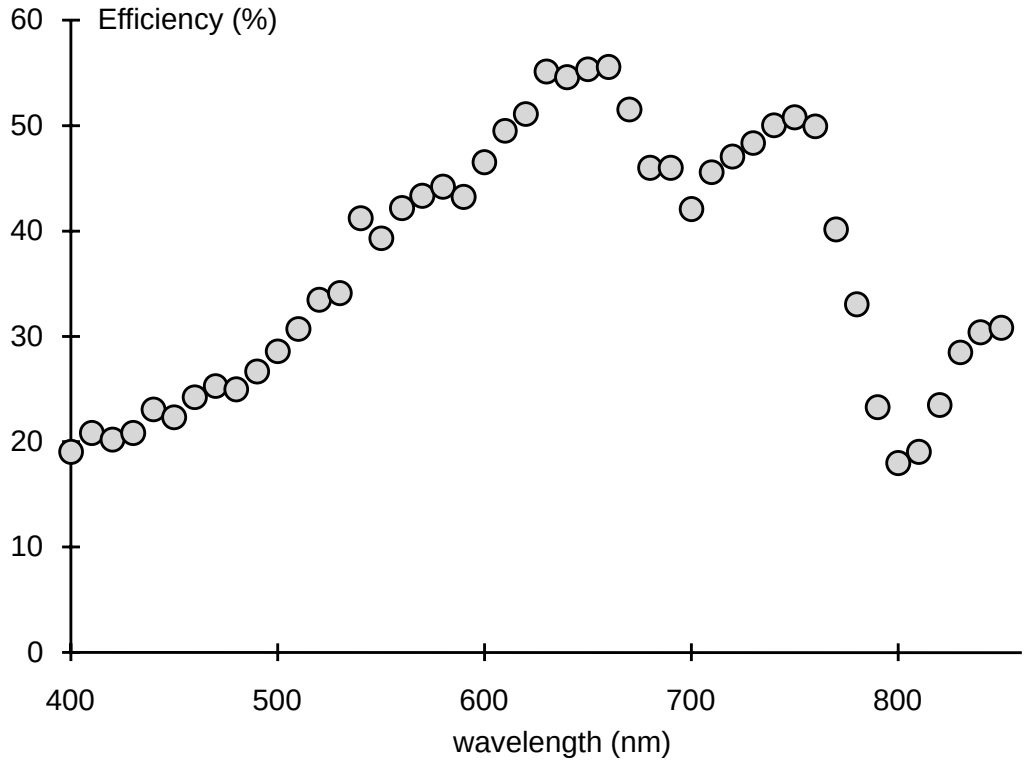

Figure 6.4: Quantum efficiency of the camera / detector system.

6.2 Lens and CCD Efficiency

The relative transmission of the camera lens was measured over a range of 400 to 800nm using the same method as described in Chapter 4 for the collimator lens. Results are shown in Figure 6.2. Full details of the testing procedures are described in Appendix B.

The sensitivity or quantum efficiency of the detector must also be taken into account. Figure 6.3 shows the sensitivity curve of the Texas Instruments TC215 CCD detector. The data was kindly supplied by Katsuo Ogura, Kokugakuin University, Tokyo.

The product of these two curves, which gives the sensitivity (quantum efficiency) of the combined camera and detector, are illustrated in Figure 6.4.

6.3 System Matrix S

The system matrix for the spectrograph, S, can now be found using the component matrices developed in previously from:

$$S = KT_3GT_2PT_1C \tag{6.4}$$

In summary of previous results:

$$C = \begin{vmatrix} 1 & 0 & F_c & 0 \\ 0 & 1 & 0 & F_c \\ \frac{-1}{F_c(1+\varepsilon_c)} & 0 & \varepsilon_c & 0 \\ 0 & \frac{-1}{F_c(1+\varepsilon_c)} & 0 & \varepsilon_c \end{vmatrix} \tag{6.5}$$

P, is equivalent to the unit matrix.

$$G = \begin{vmatrix} 1 & 2\tan\theta_b \sin\gamma & 0 & 0 \\ 0 & 1 & 0 & 0 \\ 0 & 0 & 1 & 0 \\ 0 & 0 & -2\tan\theta_b \sin\gamma & 1 \end{vmatrix} \tag{6.6}$$

$$K = \begin{vmatrix} \varepsilon_k & 0 & F_k & 0 \\ 0 & \varepsilon_k & 0 & F_k \\ \frac{-1}{F_k(1+\varepsilon_k)} & 0 & 1 & 0 \\ 0 & \frac{-1}{F_k(1+\varepsilon_k)} & 0 & 1 \end{vmatrix} \tag{6.7}$$

The translation matrices, T_1 T_2 and T_3 , correspond to component separations of 0.05m, 0.15m and 0.2m respectively. Because the prism is described by a unit matrix then T_1 and T_2 may be combined into a single translation of approximately 0.2 meters. Equations 6.4 to 6.7 can be used to calculate the system matrix, S, shown in Figure 6.5.

Note that only first order errors are included in S, with the assumption that $\varepsilon_c \times \varepsilon_k \approx 0$.

The first simplification that can be made to the system matrix is to reduce it to a 2×4 column matrix by ignoring the lower 2 rows. This is justified

$$
S = \left[\begin{array}{cccc}
\varepsilon_k - \frac{\varepsilon_k(\tau_1+\tau_2)F_k}{F_c(\varepsilon_c+\varepsilon_k)} & \varepsilon_k F_c + \varepsilon_c F_k & 2\varepsilon_k F_c \tan\theta_b \sin\gamma & \\
\frac{\varepsilon_k(\tau_1+\tau_2)+F_k(\tau_2-\tau_1)}{F_c(\varepsilon_c+\varepsilon_k)}\tan\theta_b \tan\gamma & -2\varepsilon_c F_k \tan\theta_b \tan\gamma & \varepsilon_k F_c + \varepsilon_c F_k & \\
\frac{\tau_1+\tau_2}{F_c F_k(\varepsilon_c+\varepsilon_k)} & \frac{1}{F_c(\varepsilon_c+\varepsilon_k)}\left(\varepsilon_k - \frac{\varepsilon_k(\tau_1+\tau_2)F_k}{F_c(\varepsilon_c+\varepsilon_k)}\right) & \frac{-1}{F_k(\varepsilon_c+\varepsilon_k)}\left(\varepsilon_c - \frac{\varepsilon_c(\tau_1+\tau_2)F_c}{F_k(\varepsilon_c+\varepsilon_k)}\right)\tan\theta_b \sin\gamma & -\frac{F_c+\tau_1\varepsilon_c-2\tan\theta_b \sin\gamma}{F_k(\varepsilon_c+\varepsilon_k)} \\
\frac{\tau_1+\tau_2}{F_c F_k(\varepsilon_c+\varepsilon_k)}\tan\theta_b \tan\gamma & \frac{1}{F_c(\varepsilon_c+\varepsilon_k)}\left(\varepsilon_k - \frac{\varepsilon_k(\tau_1+\tau_2)F_k}{F_c(\varepsilon_c+\varepsilon_k)}\right)\tan\theta_b \tan\gamma & \frac{1}{F_k(\varepsilon_c+\varepsilon_k)}\left(\varepsilon_c - \frac{\varepsilon_c(\tau_1+\tau_2)F_c}{F_k(\varepsilon_c+\varepsilon_k)}\right) &
\end{array}\right]
$$

where τ_1, τ_2 are the distances for translation matrices $T_{1\to 2}$ and T_3 respectively

Figure 6.5: The system matrix.

by the fact that it is only the position at which a ray strikes the image plane (detector) that is important and *not* the angle. If we define light "rays" at the object plane (fibre end) and image plane (detector) as $\vec{o}$ and $\vec{d}$ respectively, then:

$$\vec{d} = S\vec{o} \tag{6.8}$$

is now of the form:

$$\begin{vmatrix} x_{det} \\ y_{det} \end{vmatrix} = \begin{vmatrix} A_1 & A_2 & A_3 & A_4 \\ B_1 & B_2 & B_3 & B_4 \end{vmatrix} \begin{vmatrix} x \\ y \\ \phi_x \\ \phi_y \end{vmatrix} \tag{6.9}$$

The contribution to x_{det} by the element A_2 of S is in the order of $\varepsilon_k \times y$ in size. Substituting "worst case" values ($\varepsilon_k = 3 \times 10^{-4}$ from section 1 of this chapter and $y = 50 \times 10^{-6}$ being the fibre radius) then in all cases $\varepsilon_k y \leq 15 \times 10^{-9}$. With the dimensions of a single CCD pixel being almost 1000 times larger, this product and similar in elements A_1, B_1 and B_2, can be set to 0. This will also make the simplified form of S independent of the component separations. (Note, however, that this would probably be invalid if a more extended object, such as a standard entrance slit, were used instead of the fibre.)

$$S = \begin{vmatrix} \frac{-F_k}{F_c(1+\varepsilon_c)} & 0 & \varepsilon_k F_c + \varepsilon_c F_k & 2\varepsilon_k F_c \tan\theta_b \sin\gamma \\ \frac{-F_k \tan\theta_b \tan\gamma}{F_c(1+\varepsilon_c)} & \frac{-F_k}{F_c(1+\varepsilon_c)} & -2\varepsilon_c F_k \tan\theta_b \tan\gamma & \varepsilon_k F_c + \varepsilon_c F_k \end{vmatrix} \tag{6.10}$$

6.4 Image of the Fibre

The only thing left to do before the image of the fibre is calculated is to find the limits of the rays, $\vec{o}$, entering the system (refer to equations 6.8 & 6.9). These are determined by the size of the object (fibre end) and the characteristics of the collimator lens. Considering the fibre end as a small circular aperture, radius r_f, then:

$$x^2 + y^2 \leq r_f^2 \tag{6.11}$$

For a collimator lens radius (aperture/2) r_c, focal length F_c, then from the collimator matrix:

$$\phi \leq \frac{r_c}{F_c} \qquad (x, y \ll r_c) \tag{6.12}$$

The ray must then be of the form:

$$\vec{o} = \left| \begin{array}{c} x \\ y \\ \phi_x \\ \phi_y \end{array} \right| \quad , \quad \begin{array}{c} x^2 + y^2 \leq r_f^2 \\ \phi_x^2 + \phi_y^2 \leq \left(\frac{r_c}{F_c}\right)^2 \end{array} \tag{6.13}$$

Once the appropriate constants are substituted, equations 6.13, 6.9 and 6.10 can be used to calculate the images in the form of “spot" diagrams. This was done for the paths of approximately 24,000,000 rays. At the detector each ray contributed 1 “photon" at the position defined by x_{det} , y_{det}. The photons were binned and stored in a large array of $\frac{1}{2}\mu^2$ pixels to get the final image of the fibre end.

Figures 6.6 to 6.9 are the calculated images with the size of a single $12\mu \times 12\mu$ CCD pixel shown as a small white square in the lower right of each image. The dispersion direction is horizontal and cross-dispersion vertical. The circle in Figure 6.6 represents the size of the fibre image if there was no distortion caused by the echelle grating.

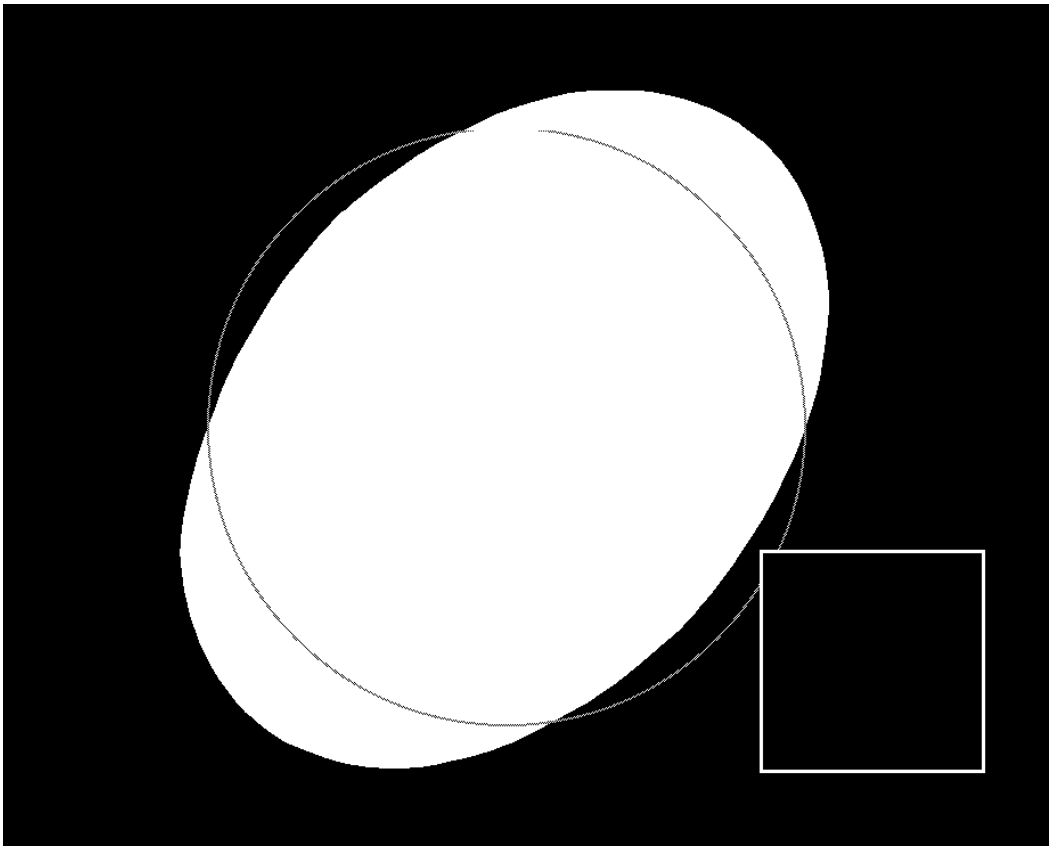

Figure 6.6: Image of the fibre with $\varepsilon_k = \varepsilon_c = 0$.

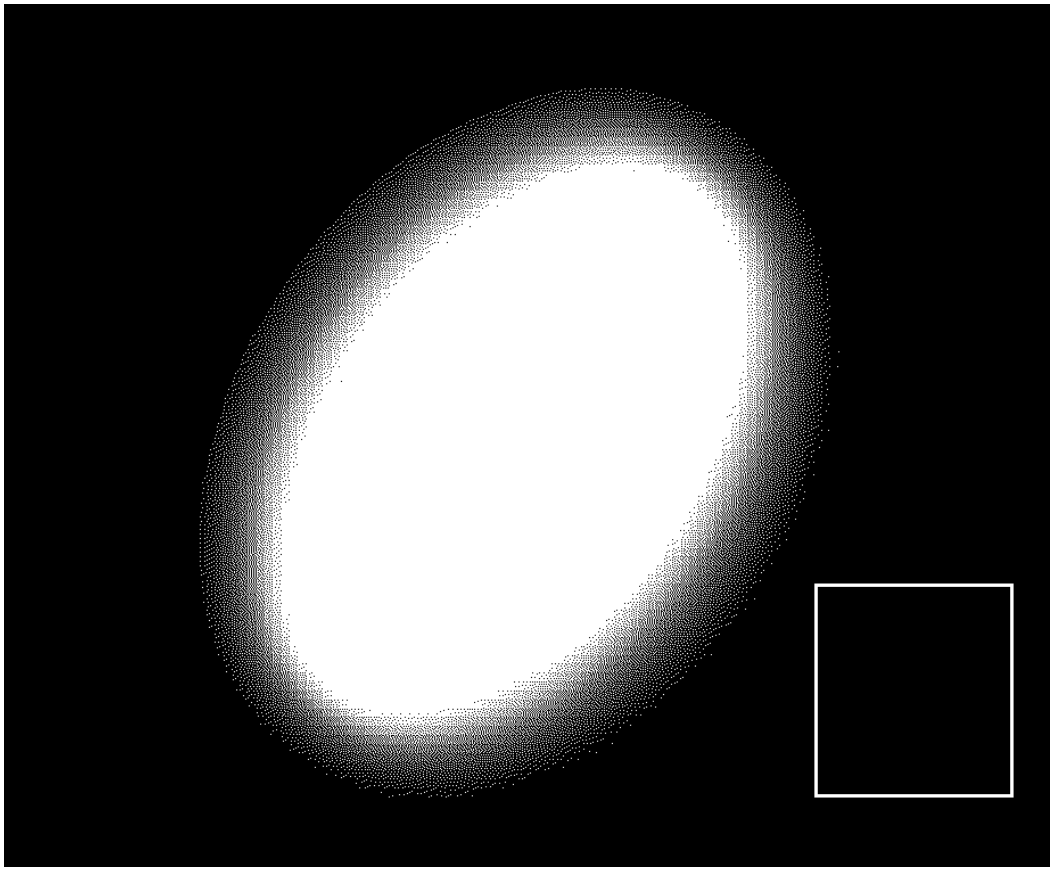

Figure 6.7: Image of the fibre with $\varepsilon_k = \varepsilon_c = 1 \times 10^{-4}$.

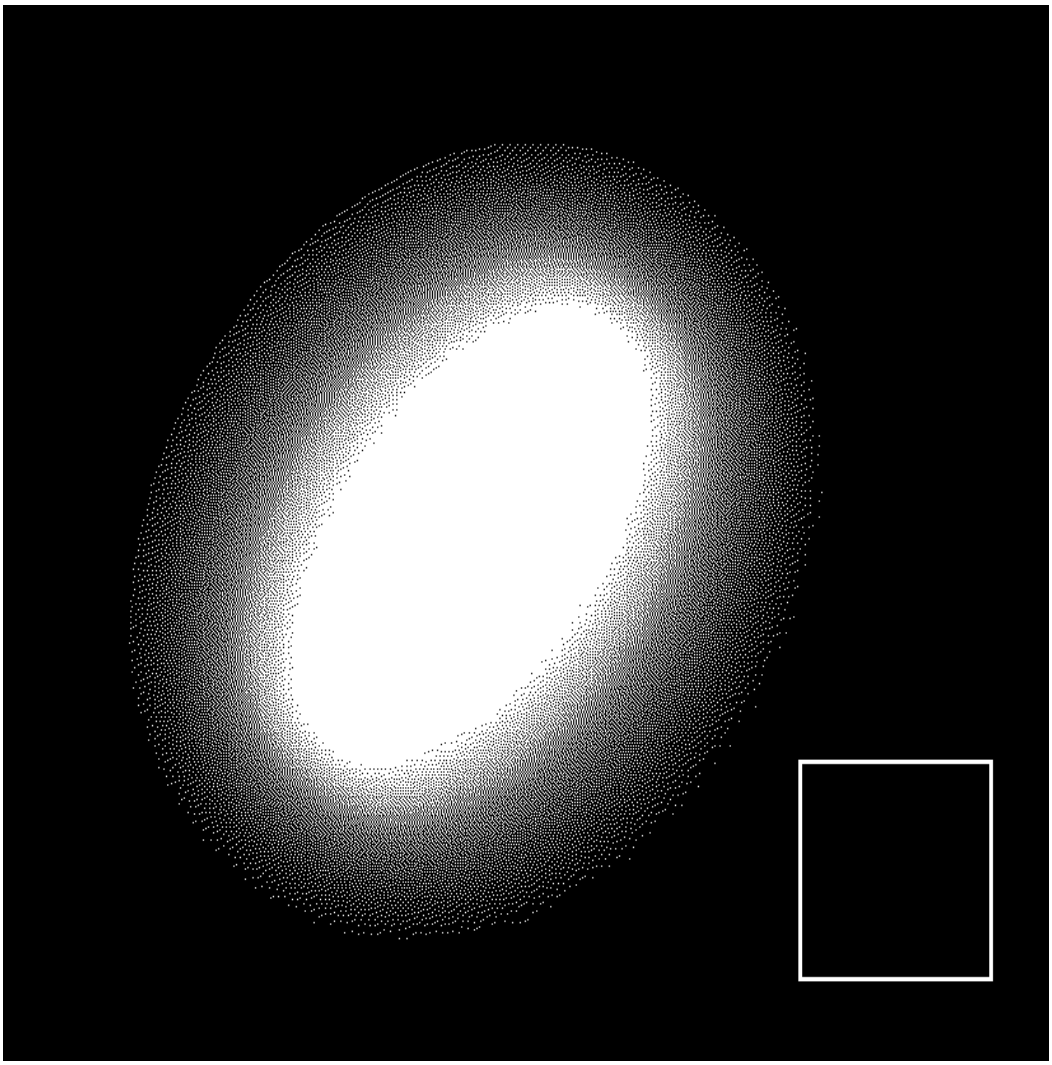

Figure 6.8: Image of the fibre with $\varepsilon_k = \varepsilon_c = 2 \times 10^{-4}$.

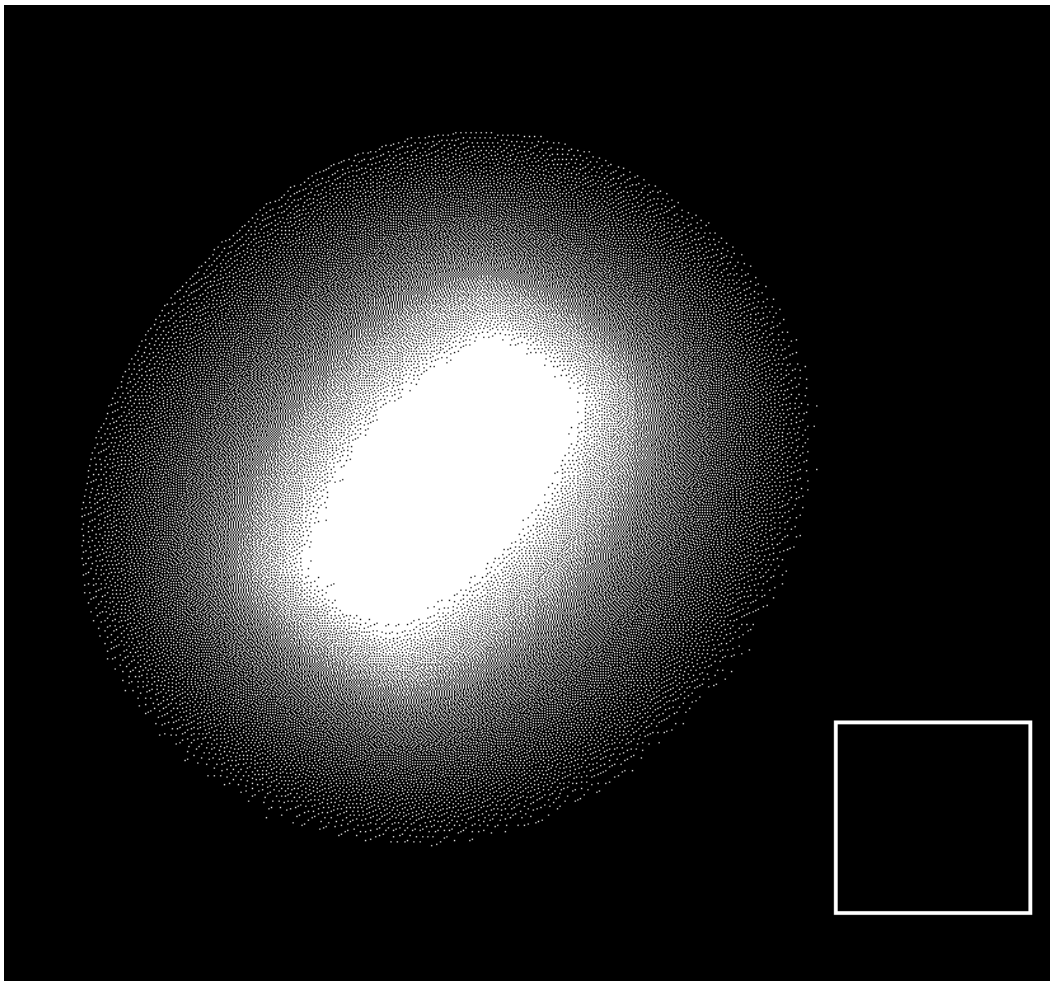

Figure 6.9: Image of the fibre with $\varepsilon_k = \varepsilon_c = 3 \times 10^{-4}$.